Review Article

Pengfei Zhang*, Zongxing Wang, Junru Li, Xinlin Li, and Lianjun Cheng*

From materials to devices using fused deposition modeling: A state-of-art review

Abstract: Fused deposition modeling (FDM) uses computer-aided design to direct a 3D printer to build successful layers of product from polymeric materials to generate 3D devices. Many reviews have been reported recently on the cutting-edge FDM technology from different perspectives. However, few studies have delved into the advances in FDM technology from materials to 3D devices. Therefore, in this work, with a bottom-up approach from materials (including commodities and nanomaterials) to printing process (including effort for fast printing, effort for resolution improvement, and simulations) and from printing process to 3D devices (including biomedical implants, topological structures, and multifunctional devices), it aims at reviewing the FDM technology developed over the past decades.

Keywords: FDM, nanomaterials, 3D structures, simulations, high performance

Nomenclature:

ABS   –   acrylonitrile butadiene styrene
HA   –   hyaluronic acid
HDPE   –   high-density polyethylene
HIPS   –   high impact polystyrene
LCP   –   liquid-crystal polymer
LDPE   –   low-density polyethylene
PAI   –   poly(amide imide)
PBI   –   poly(benz imidazole)
PC   –   polycarbonate
PCL   –   polycaprolactone
PEEK   –   poly(ether ether ketone)
PEI   –   polyethylenimine

PI   –   polyimide
PLA   –   poly(lactic acid)
POM   –   polyoxymethylene
PP   –   polypropylene
PPE   –   poly(p-phenylene ether)
PPO   –   poly(p-phenylene oxide)
PPS   –   poly(phenylene sulfide)
PS   –   polystyrene
PSU   –   polysulfone
PU   –   polyurethane
PVA   –   poly(vinyl alcohol)
PVC   –   poly(vinyl chloride)
SAN   –   styrene-acrylonitrile resin
TPU   –   thermoplastic polyurethane
UHMWPE   –   ultra-high-molecular-weight polyethylene

1 Introduction

Additive manufacturing, which is distinguished from subtracting manufacturing, uses computer-aided design to direct a 3D printer to build successful layers of product from powder, molten plastic, or other materials to generate 3D devices. As summarized in some excellent reports, there are numerous advantages of applying the state-of-the-art additive manufacturing in science and engineering research. After reviewing the current and emerging approaches in hydrogel design and bioink reinforcement techniques, Gaharwar and coworkers [1] confidently concluded that additive manufacturing is one of the successful methods for developing next-generation cellularized 3D scaffolds to mimic anatomical size, tissue architecture, and tissue-specific functions. Plocher and Panesar [2] pointed out that, in conjunction with mathematically based structural optimization approaches, the additive manufacturing provides a portfolio of solutions for next-generation lightweight structures. Culmone and coworkers [3] summarized various 3D printing methods in the field of medical devices. After examining the reasons behind choosing additive manufacturing technology to produce instruments for diagnostics and surgery, they

* Corresponding author: Pengfei Zhang, School of Electromechanical Engineering, Qingdao University, Qingdao, Shandong 266071, China, e-mail: pzhang@qdu.edu.cn
* Corresponding author: Lianjun Cheng, School of Electromechanical Engineering, Qingdao University, Qingdao, Shandong 266071, China, e-mail: chenglianjunwp@163.com
Zongxing Wang, Junru Li: School of Electromechanical Engineering, Qingdao University, Qingdao, Shandong 266071, China

concluded that additive manufacturing opens a door to a new approach in the production of medical devices, allowing the complexity of designs to be pushed to the extreme. Some other works have been carried out with interest in summarizing the applications of additive manufacturing in construction [4], aerospace [5], and polymer–fiber composites [6], just to name a few. Kim and coworkers [7] reviewed advanced quality control technology in the additive manufacturing process. To conclude, all sorts of products can be produced with a 3D printing, from medical implants to auto and aircraft parts, batteries, energy harvest devices, and commercial accessories for mobile phones. The printing process requires as little as 10% of the raw material expended in traditional manufacturing (i.e., subtracting manufacturing) and uses less energy than conventional factory production. What's more, a 3D printer can print multiple copies just like a photocopy machine and run-off three-dimensional products with precise dimensions. Therefore, the development of 3D printing techniques would enable each individual potentially be their own manufacturer as well as their own internet site and power company. Because of those extraordinary benefits, the 3D printing technology has been hailed as the new infrastructure for a Third Industrial Revolution.

Among those developed additive manufacturing methods and practical applications, fused deposition modeling (FDM) has been well-adopted in multiple applications as a 3D printing technology in prototype or end-product [8–10]. During FDM printing process, polymeric material is sent to the nozzle through a wire feeding device, after which a heater converts the material from solid to molten state, and then the molten material is extruded by a nozzle onto a base plate. The nozzle moves horizontally on X–Y plane. After the completion of layer deposition, the base plate moves in a vertical direction. It descends a thickness of one layer in a predetermined increment. Then it continues the fused deposition until the entire 3D shape is completed. It is worth noting that, when printing, each layer is printed with a contour first and then with an internal filling, for the sake of saving printing time. The nozzle moving speed, temperatures, and layer height setting of the first layer at the start of printing are different from those of the other layers. The difference in the settings is highly recommended. This is because it can enhance the adhesion between the sample and base plate, further to prevent warpage.

FDM has become a more mature 3D printing method. Many reviews have been reported recently on the cutting-edge FDM technology from different perspectives. However, few studies have delved into the advances in FDM technology from materials to 3D devices. In this review work, it aims at reviewing the cutting-edge FDM technology developed over the past decades, with a bottom-up approach from materials (including commodities and nanomaterials) to printing process (including effort for fast printing, effort for resolution improvement, and simulations) and from printing process to 3D devices (including biomedical implants, topological structures, and multifunctional devices), explicitly demonstrated in Figure 1.

2 Materials

Thanks to the improvement advances in FDM printing technologies, especially the Arburg Plastic Freeforming [11], the choice of polymeric materials has increased considerably to a wide range for FDM printer. These materials have to meet at least two criteria: (1) relatively low melting temperature (T_m) and (2) appropriately high glass transition temperature (T_g). This is because low T_m makes the 3D printing more affordable; while with a high T_g the polymer could solidify fast enough after the extrusion so that the shape can be held as printed [12–14]. It is worthy to mention that T_g is a property of the amorphous materials or the amorphous portion of the semicrystalline [15]. When the ambient temperature is below T_g, the molecular chains of amorphous materials or the amorphous phases are frozen in place, behaving like solid glass.
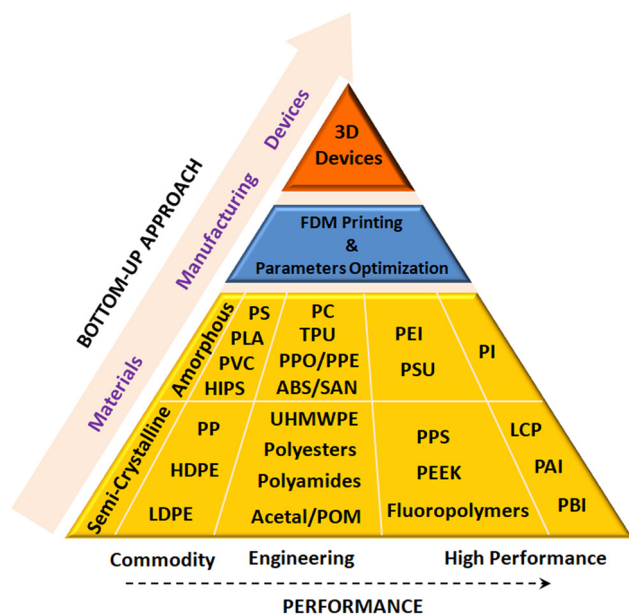
Figure 1: Bottom-up approach from materials to devices using FDM.

Figure 1 shows plenty of polymeric materials suitable for FDM technology from commodity to engineering and from engineering to high performance polymers, such as PCL for topological self-interlocked structures [16–18], UHMWPE for artificial implant [19], nylon for lightweight structure based on polymeric alloys [20], PVA for medicine device [21], PU for energy absorber [22], elastomer Tangoblack for self-powered triboelectric touch sensor [23], PC for food and/or drug packaging and medical devices [24], PEEK for biomedical implants (such as bulk implants, orthopedic implants, prosthesis systems, just to name a few) [25–30], so on and so forth. It is worth noting that the listed materials in Figure 1 are all pure polymers, which provide great potentials for FDM end-products. However, some of them are facing challenges when used in FDM process. To overcome those challenges, different types of fillers have been proposed to the rapidly developed market, such as particles, fibers, and nanomaterials [31].

2.1 Particle-reinforced polymeric materials for FDM

When applied to FDM printing process, challenges faced by some of the polymeric materials include: (1) the printing wire is easy to break and thus the extrusion is not smooth; (2) the molded FDM parts are easy to warp and thus they have insufficient strength and low surface quality. Therefore, particles have been added to pure polymers with the aim of improving the rheological behavior and thus enhancing the mechanical properties, or improving the surface quality of FDM products. For instance, Wu and coworkers [32] applied the organo-modified montmorillonite (OMMT) to poly(L-lactide) (PLLA) to improve the rheological behavior of PLLA. It pointed out that OMMT were uniformly dispersed in the PLLA matrix in intercalation mode, and also the dispersed OMMT acted as a heterogeneous nucleating agent to promote the crystallization of PLLA. Tao and coworkers [33] added wood flour to PLA matrix. The results showed that the wood flour has changed the microstructure of material fracture surface, and the initial deformation resistance of the composite was enhanced as a result. Daver and coworkers [34] made a bio-interpretable cork-PLA by combining cork with PLA and adding tributyl citrate as a plasticizer, improving the elastic modulus and strength compared to pure PLA. Metal particles have also been used as fillers to FDM polymeric filaments [35]. Nikzad and coworkers [36] added different volumes

of metallic fillers such as iron or copper powder to ABS to make iron/ABS or copper/ABS composite. It was found that with the increase of metallic content in the composites, the tensile strength, flexural strength, and impact strength of the composites are lower than those of pure ABS materials, but the thermal properties have been significantly improved, leading to better surface quality.

2.2 Fiber-reinforced polymeric materials for FDM

Other issues faced by polymeric materials include the lowest interlaminar bonding strength and the highest mechanical anisotropy [37]. Thus, by modifying the polymer matrix with fillers, more isotropic and stronger FDM parts have been achieved. Quan and coworkers [38] mixed short carbon fiber (SCF) with ABS, which reduced the porosity of the molded sample and further improved the mechanical properties as well. When the SCF content was 30%, the tensile deformation of the molded sample strength and tensile modulus increased by 52% and 378%, respectively. Galatas and coworkers [39] printed ABS film first and then combined the film with a carbon fiber fabric to create a sandwich structure for strength and modulus improvement. Compared to pure ABS samples, the ultimate strength and Young's modulus of the sandwich structure were improved tremendously. For instance, the ultimate strength improved about nine times and the Young's modulus increased about 16 times. Gao and coworkers [40] explored the relationship between fillers and properties of FDM parts by adding different volume fillers (carbon fiber or talc powder) to PLA. They found that the filler has a significant effect on the formation of interlaminar bonding of FDM parts.

2.3 Nanomaterials for FDM

Nanomaterials are defined here as polymer matrix-based nanocomposites for FDM 3D devices. The nanoparticle inclusions are taken as the important potential fillers for enhancing physical and mechanical properties of polymer matrix. These inclusions include exfoliated clay, carbon nanotubes, carbon nanofibers, exfoliated graphite, nanocrystalline metals, and a host of additional nanoscale inorganic filler [41–47]. Once incorporated into polymeric matrix, as shown schematically in Figure 2, the types of morphology are usually categorized into three

(a) Immiscible dispersion   (b) Intercalated dispersion   (c) Exfoliated dispersion
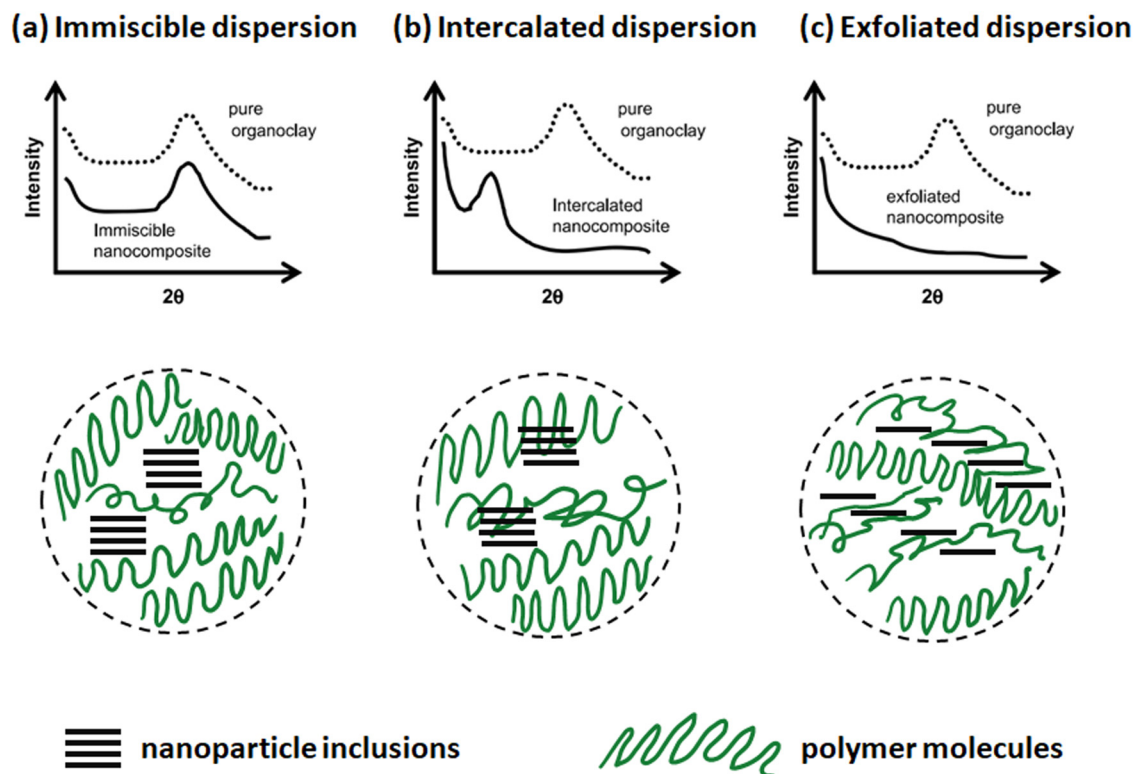
Figure 2: Schematic illustration of different states of dispersion of nanoparticle inclusions in polymeric matrix with corresponding WAXS: (a) immiscible; (b) intercalated; (c) exfoliated. Adopted from ref. [48,49] with modification.

states: immiscible, intercalated, and exfoliated (miscible). For the sake of properties enhancement, complete exfoliation of nanoparticle inclusions is highly desired after the incorporation process.

Studies have been taken to develop nanomaterials for FDM with prospect to overwhelm the property or performance restrictions of traditional/conventional materials. For instance, Liu and coworkers [50] developed polymer matrix composites with carbon nanotubes and graphene nanoplatelets for FDM. The tensile test of FDM-printed dogbone (according to ASTM D638) showed that the mechanical property in the filament-oriented direction has been enhanced due to the incorporation of nanoparticles. Similar results have been reported in the references, showing mechanical property improvement in filament-oriented direction [51–55]. As explained in the Figure 2, complete exfoliation of nanoparticle inclusions would improve the mechanical property of filament. It would not be surprised to acknowledge the improvement of mechanical property in the filament-oriented direction. However, in the perpendicular direction, it is hard to improve the mechanical property by using nanoparticle inclusions. This is because the interfacial bonding between two adjacent printed layers plays

a significant role in determining the properties in the perpendicular direction (i.e., normal to the filament orientation direction). During the formation process of interfacial bond, it undergoes stages from surface contacting, neck growth to molecular diffusion [56]. It is seldom to see the work on using nanoparticle inclusions to improve the surface contacting, neck growth, or molecular diffusion during FDM process.

Many other works have been reported to improve the processing or performance of 3D devices by using nanoparticle inclusions. Cobos and coworkers [57] added multiwalled carbon nanotubes (MWCNTs) and halloysite nanotubes to PLA matrix with the aim of improving its thermal properties. But because of the cluster of nanoparticles, defects exist within filaments if printed at a high scanning speed. In their work, maleinized linseed oil was added to the nanocomposites as plasticizer to mitigate the defects. It showed that the melt flow index increased approximately 46% from the capillary rheometry results. Bronze nanoinclusion was introduced to PLA matrix to improve the tribological properties of 3D-printed devices, enabling them owning unique performance such as self-lubrication, vibration-damping, and corrosion resistance [35,58]. Also, graphene (GnP) filler

was widely used in FDM to improve the dielectric and/or electromagnetic interference shielding properties of the printed devices [51,59–65]. Since temperature gradient within a nozzle during printing process plays a great effect on the printing speed and product properties, great attention was paid to improve the thermal properties of polymeric filament, using cellulose nanofibrils [52], graphene nanoplatelets [66], graphene oxide [67], and MWCNT [68]. In addition, nanofillers have been used to improve the antibacterial and biocompatible performance of FDM-printed implants [69,70].
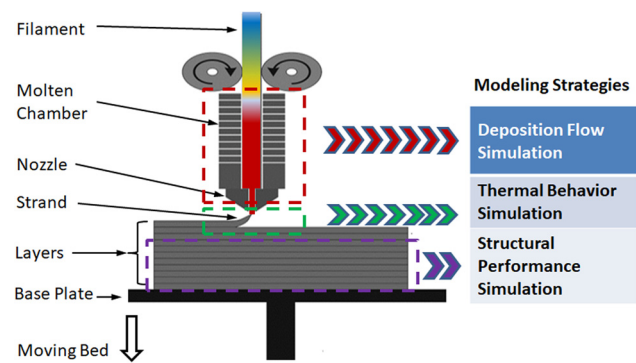
Figure 3: Schematic of simulation strategies for FDM process.

3 FDM printing

If the performance of a material determines the upper limit of the printed devices, appropriate setting of process parameters is an effective strategy to achieve the upper limit of the performance. There are a number of great work published on reviewing process parameter influences and optimization for FDM process [8,71–73]. The parameters of FDM could be divided into four categorizes, including temperature, hierarchical, speed, and raster. However, how to optimize these parameters is not our interest in this work.

FDM prints functional devices using extrusion nozzles with about 0.1–1 mm width scales. FDM-like technique uses nozzles with centimeter width [74]. The Big Area Additive Manufacturing system, also with centimeter-width scale nozzles, can print 3D structures on the order of several meters [75]. Despite the record of high extrusion rate, solving the rate-resolution tradeoff problem is essential to accelerate the FDM adoption and industrialization.

3.1 Effort for fast printing

Since the first commercial FDM system sold by Stratasys, they are all gear-driven extrusion-based 3D printers. Filament is fed by gears into a chamber, where the filament is melted completely, as shown in Figure 3. The applied shearing force between the filament and gears drives melted polymer flowing through a nozzle. By multiplying the cross section area of the nozzle and extruding speed, it gives the extrusion rate. Nowadays, the size of a FDM filament becomes standard with a diameter of 1.75 mm. According to the law of conservation of mass, the extrusion rate of a FDM printer is mainly determined

by the gear feeding speed. Efforts have been taken to increase the gear feeding speed, as shown in Figure 4, for the purpose of improving the extrusion rate and further increasing FDM printing rate [76,77]. For instance, a motor shaft (large circle) pinches filament against a ball race (small circle), driving it down through the chamber and pushing it out through a nozzle, as shown in Figure 4(b). Figure 4(c) shows another solution for increasing pinch force, thereby improving the filament feeding speed. Given the circumstances of intrinsic high resistance of thermal penetration of polymeric filament, however, higher filament feeding speed would result in a higher risk for extruder clicking, gears slipping, and nozzle clog [78].

Go and coworkers [79] have pointed out that an FDM printer can't print at a higher rate than the one dictated by its rate-limiting module; otherwise failure of a single module would occur, resulting in failure of the process altogether. This is because, for a given extrusion rate, the extruder must feed the filament at a commanded velocity, while providing sufficient force to overcome the flow resistance in the chamber. The chamber, in turn, must be capable of heating the filament to the target temperature at a specified heating rate. The motion system must then move the printhead (the extruder and chamber) at a rate commensurate to the exit velocity of material from the nozzle. Thus, they proposed a solution for fast printing, as shown in Figure 5. In addition to a conventional heating block within the printhead, a laser heating element was mounted on purpose, which ensures the melting of polymeric filament prior to entering the chamber (conventional heater block). They also proposed to use threaded filament rather than using regular filament products to increase extrusion force. The shear engagement area between filament and textured driving wheel has been remarkably increased [76]. As a result, the designed printhead was able to extrude materials at a
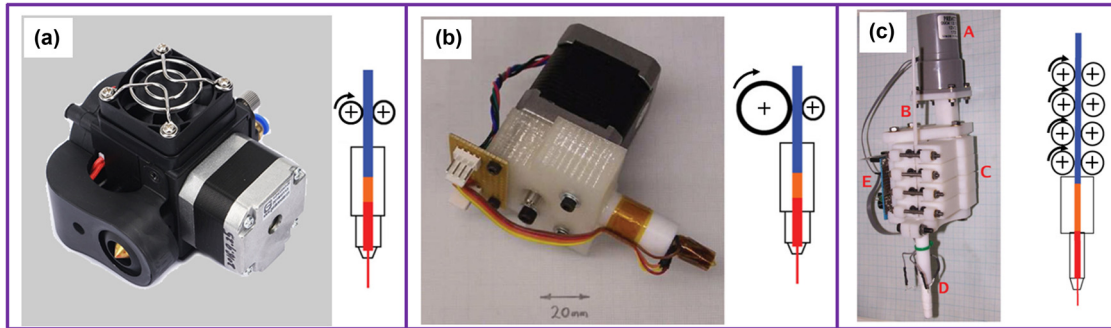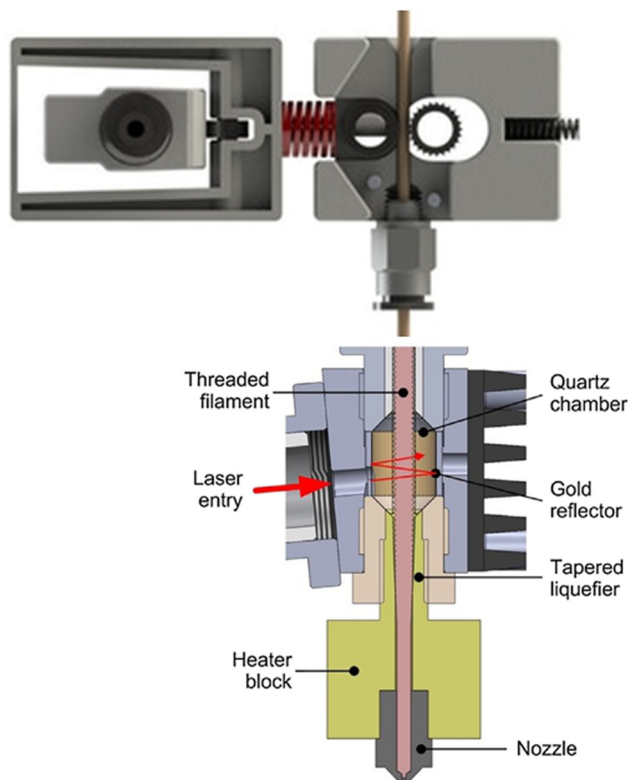
Figure 4: Gear-driven extrusion-based nozzles for FDM printers: (a) drive gear having same diameter size as bearing roller; (b) drive gear having larger diameter size than bearing roller; (c) multiple drive gears and bearing rollers but drive gears having same diameter size as bearing rollers. Adopted from ref. [76] with modification.

rate of 141 cm³/h for a 0.5 mm nozzle. The extrusion force approached up to 160 N. As compared, a commercial FDM printer (Stratasys Mojo, as shown in Figure 4(a)) prints a 3D structure at a volumetric infill rate of 21 cm³/h for a 0.5 mm nozzle, corresponding to an estimated extrusion force of 30 N.

The proposed laser-assisted printhead can print 3D devices with nozzle diameters of 1.0 and 0.5 mm. It has been approved that the printhead owns fast printing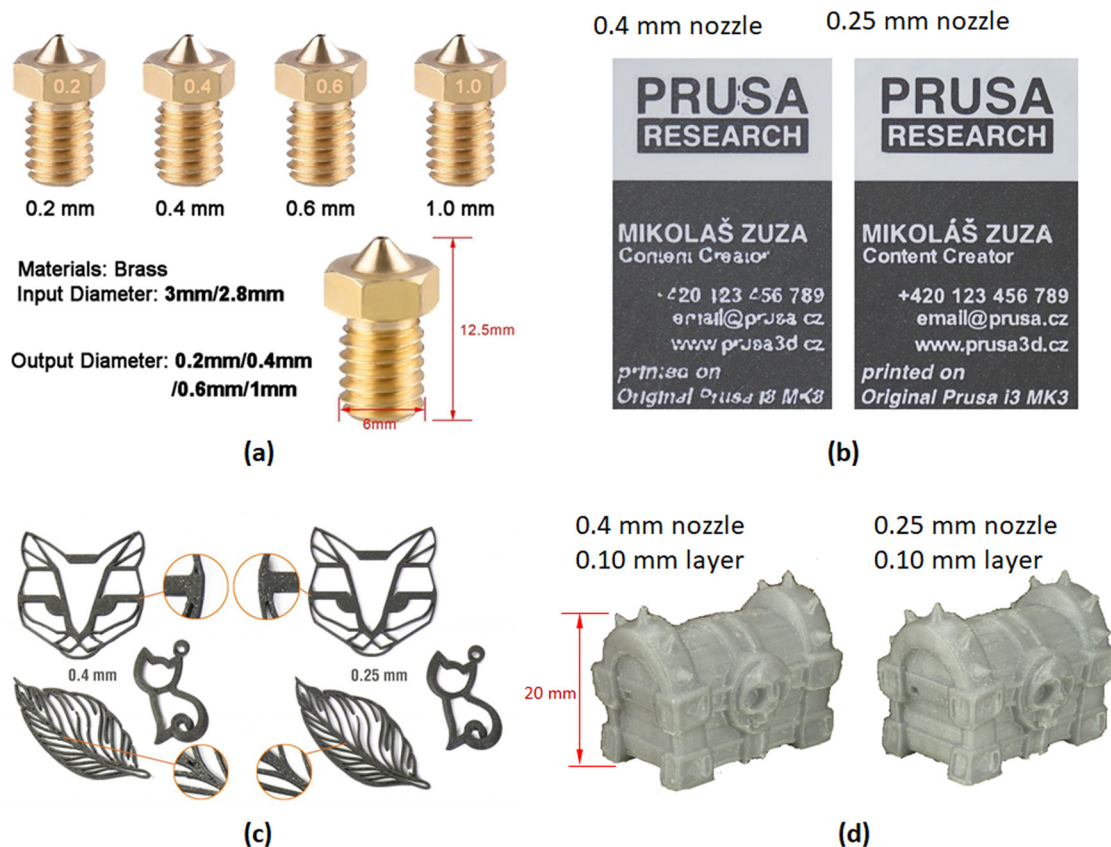 capability. However, can it still print fast if the nozzle diameter goes smaller than 0.5 mm? Besides, the FDM printing resolution in the *XY* axis is significantly greater (≈300 ηm) than what can be achieved with other techniques, such as SLA (≈10 ηm) and inkjet (≈50 ηm) [81]. An essential question for FDM printing is whether it can be made to extrude ever-smaller filament to achieve the micro-sized features that are desired for so many applications.

3.2 Effort for resolution improvement

In 3D printing, resolution is the quality, or level of details, at which the product is created. Higher resolution value means more printing details. In general, by using FDM, the movement of printhead on both *X–Y* and *Z* planes determines how fine the resolution would be. At its most basic level, the *X–Y* resolution is controlled by the size of nozzle and the movement of printhead. But for *Z* resolution, heat is the dominant factor in determining the outcome. This is because, due to heat transfer, a small layer height will distort previous layers. In this review work, it mainly focuses on the efforts for *X–Y* resolution improvement. In Figure 6, it shows typical FDM nozzles with different sizes as well as examples telling the resolution difference between 0.25 and 0.4 mm nozzles. Obviously, smaller nozzle gives higher printing resolution (i.e., more detailed prints). But, with a smaller nozzle size (0.2 mm diameter, for example), drawbacks of the printing process are blocking and buckling and even slippage of the wire on the pinch wheel [82]. This is because the filament is extruded to a very tight diametric tolerance with a gear-driven-based nozzle. A variation in filament diameter may cause blocking and/or slippage of the wire on the pinch wheel.

Figure 5: The feeding of threaded filament and the laser-assisted heating chamber. Adopted from ref. [80] with modification.

Figure 6: (a) Typical commercial FDM nozzle with different sizes; (b) FDM printed texts with different nozzle sizes; (c) FDM printed jewelry with different nozzle sizes; (d) FDM printed miniatures with different nozzle sizes. Adopted from ref. [83] with modification.

One of the great issues resulting from small nozzles is the build up of backpressure against the filament extruding. Regular solutions to this problem are either to print at a low speed or to avoid using small nozzles. At higher printing speed, the backpressure builds up by the geometry of nozzles. Thus, high speed printing is usually not suggested when using a nozzle with small size. Efforts have been made to overcome these challenges. Silveira and coworkers [84] proposed an interchangeable nozzle based on mini screw extrusion for the sake of fast printing when using a 0.4 mm nozzle. The difference between a commercial FDM nozzle and screw-based nozzle is shown in Figure 7. In Figure 7(a), the filament is driven by pin wheels and extruded through the nozzle at a relatively low speed, ensuring to be completely melted within the chamber. As shown in Figure 7(b), a mini screw extrusion-based FDM nozzle unit consists of a nozzle, screw, and barrel as well as peripherals. The printing material is driven forward by a mini screw, but extruded through the nozzle at a relatively high speed. By extruding PCL, the extruding rate has been improved to 65 cm^3/h. After an optimization on configuration

of screw section and screw geometry, the extruding rate has been greatly improved to 167 cm^3/h for PEEK [85]. The configuration and geometry of screw-based FDM nozzle unit are illustrated in Figure 7(c). However, the disadvantage in screw-based nozzle unit is that it requires several types of heaters surrounding the barrel in order to ensure a complete melting. Consequently, the weight of a mini screw extrusion-based FDM nozzle is much higher than a filament-based nozzle. Because of the heavy weight, it leads to a large inertial force during a printing process, resulting in a difficulty in the control of printing accuracy [86–88].

It is worth noting that die swell exists during both filament-based and screw-based FDM. It occurs when non-Newtonian fluid flows in the mold in the extrusion process. Due to the shear stress formed along the die wall, the polymer chains align with the flow direction. When they reach the nozzle outlet, constraints disappear, and thus, because the conformational entropy tends to increase, these chains are driven to return to their original and misalignment state, resulting in the increase of volume (i.e., extrudate diameter) [89]. As a result, the
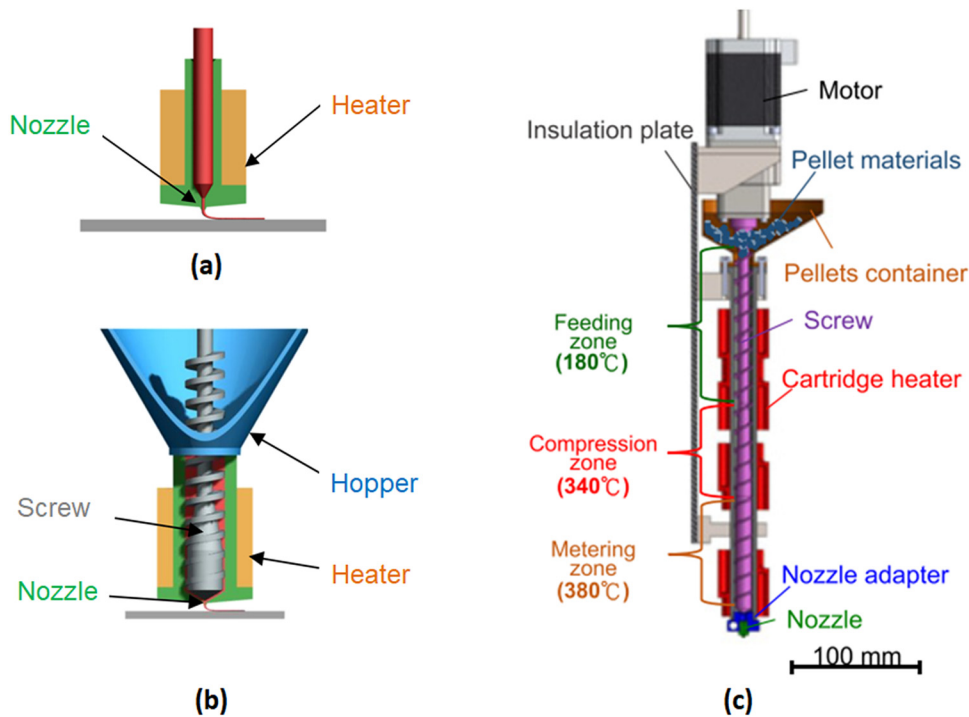
Figure 7: (a) Filament-based FDM nozzle; (b) screw-based FDM nozzle; (c) configuration and geometry of screw-based FDM nozzle unit. Adopted from ref. [85] with modification.

size of the extrudate is larger than that of the die. The shape of the cross section also changes when non-Newtonian fluid is forced to extrude the exit die. To date, as reported, the smallest nozzle diameter was 0.15 mm. Although it has been claimed that FDM printer can print an object of 50 microns or even higher, it is of great importance to note that the claimed resolution is limited on a Z-axis. Due to die swell, the resolution or printing width on $X–Y$ axis never reaches to 0.15 mm or higher. How to avoid die swell for FDM becomes a challenging question.

Electrohydrodynamic-based FDM (E-FDM) was proposed for the easy manufacturing of high-resolution patterns with sub 10 μm, by generating micro-scale liquid extrudate via the application of a high voltage between the nozzle and substrate, as shown in Figure 8. With this strategy, die swell has been well-avoided when printing high-resolution FDM products. The working principle is similar to that of electrospinning [90–92]. The difference is that the fibers formed in the electrospinning process are quite randomized and thus the fiber orientation could not be controlled precisely. However, in the E-FDM process, the fiber orientation can be controlled precisely and thus finest 3D structures could be printed [93].

The printed pattern stability and resolution are influenced by E-FDM parameters including temperature, feed-rate, pressure, voltage, plotting speed, and nozzle size [92,94]. Temperature is a unique factor that impacts the viscosity. In one of the studies, a temperature range from 235°C to 260°C was investigated for PLA material. As being pointed out, when temperature reached over 250°C, stable cone-jet becomes more difficult to maintain and resolution fluctuates more significantly [91]. Definitely, there is a critical point in the temperature range; in other words, the pattern and resolution can be improved when temperature increases as long as it is below the critical point. There is also a critical point for voltage and plotting speed [90]. With fixed voltage and plotting speed, higher pressure leads to stable jet and skewed cone-jet. Better printing resolution could be obtained with smaller nozzle size and lower feed-rate [95]. Currently, only PCL and PLA have been reported for biomedical devices by E-FDM. For instance, Wang and coworkers [94,95] fabricated controlled uniform 3D porous PCL scaffolds using E-FDM towards the realization of printing functional human organs. He and coworkers [92] constructed high-resolution nanoscale patterns by simply controlling the movement of E-FDM collector according to a user-specific program. Wu and coworkers [96] produced controllable caplets for personalized medicine using E-FDM for the sake of safety and efficacy of the drug delivery system.
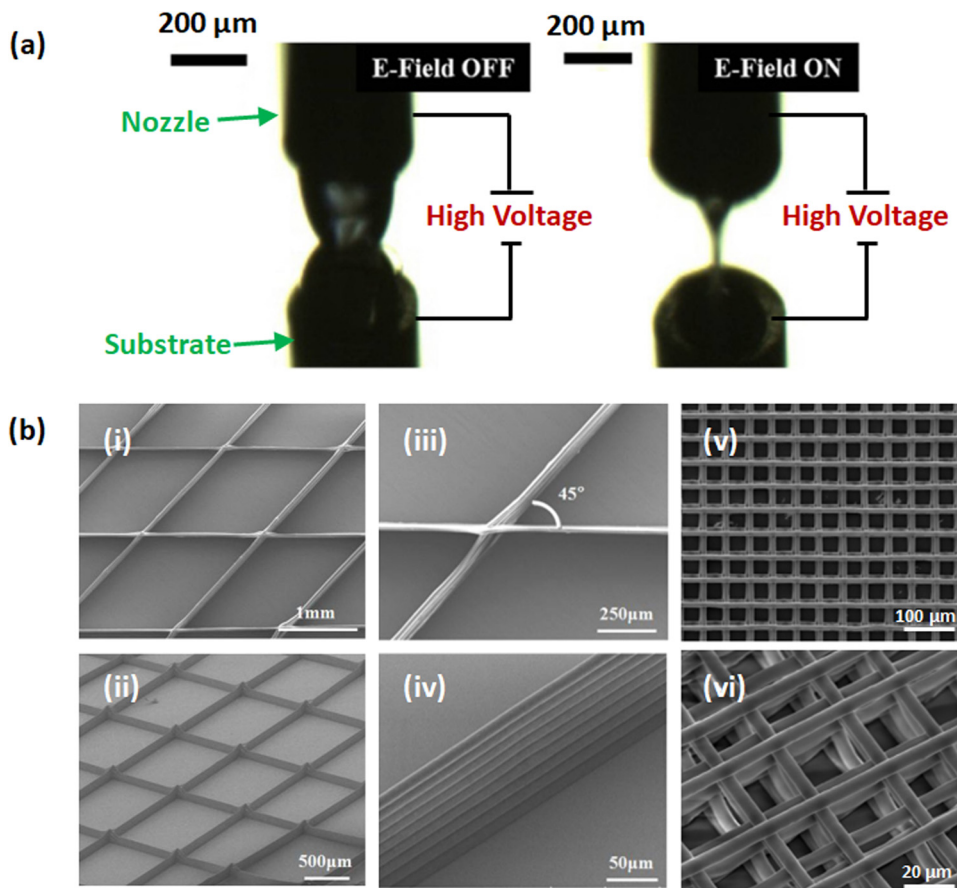
Figure 8: (a) Electric field OFF/ON effect on E-FDM printing; (b) E-FDM-printed 3D scaffold structures. Adopted from ref. [90–92] with modification.

3.3 Simulation

Simulation is especially important for high-value components fabricated using the state-of-the-art 3D printing process. It helps to understand and visualize the complex thermomechanical phenomena taking place during 3D printing. For instance, through a numerical simulation on mixture of PLA-nHA, Li [97] successfully printed out FDM biomimetic artificial bone to meet the accuracy requirements of clinical bionic artificial bone replacement. Thus, it is highly important to take simulation strategy to understand the FDM processing by establishing simulation models from deposition flow to thermal behavior to structural performance, as shown in Figure 3.

3.3.1 On feeding process

On the feeding process, filament is fed into a chamber, in which it undergoes a reversible transition from solid to liquid. A lot of works have been carried out to understand the rheology of polymeric materials by using different statistical and heuristic methods [71]. With the aim of processing parameter optimization, these simulation works mainly focused on identifying key processing parameters by studying the thermal and thermomechanical behavior of the printed part, postdeposition of the feeding process. According to analytical or numerical thermal models, the relationship between printing-process parameters and thermomechanical behavior could be established for better controlling product quality [98–100].

The feeding process involves multi-physics (including thermal and dynamic) phenomena on different spatial and temporal scales. It is worth noting that the extrusion is a local operation while the printing of an entire product is a global process. Physically sound models based on numerical simulations have been conducted to understand the feeding process and to gain parameter optimizations [101,102]. For instance, computational fluid dynamics (CFD) simulations of the deposition flow were proposed to

predict the flows of melted filament inside the molten chamber, including the calculation of flow field, pressure drop, and melting distance to the entry of the chamber [103]. With CFD model, the impact of feeding process on dimensional accuracy and mechanical properties of the final product was thoroughly investigated. It found that the shape of printed strand can be affected by feeding rate, nozzle dimensions, and extruding force. Furthermore, the shape has a direct impact on the surface roughness of the printed part, cooling efficiency after the printing, and the interfacial bonding strength between adjoining strands and overlaid layers.

3.3.2 On interfacial bonding

After deposition process, the strand undergoes a transition from liquid to solid. Fast cooling of the printed strand causes solidification prior to the complete molecular interdiffusion with other strands, leaving voids or defects between adjoining strands and overlaid layers that do not have full mechanical properties [18]. As been pointed out, thermal behaviors of the filaments after deposition significantly determine the quality of the FDM 3D product [104]. This is because, during the formation of interfacial bonds, temperature profiles are involved in all interface wetting, molecular diffusion, and randomization [105]. As temperature profile being involved, the polymer chains continue to diffuse with an increase in the mechanical properties of the interface. Therefore, it is crucial to establish analytical models to predict thermal history of a strand after deposition.

There are a great number of excellent work reviewing the simulation tools for predicting thermal history of strands under FDM extrusion [106–108]. Here, we categorize them into three groups: (1) the one-dimensional transient heat analysis (1D THA), which only accounts for either the strand width or the layer height due to the one-dimensional limitation [109]. (2) The two-dimensional transient heat analysis (2D THA), with which the strand has a rectangular cross section. Accordingly, the effect of conduction to the platform can be neglected and any contact resistance between strands could be negligible [110–112]. (3) The three-dimensional transient heat analysis (3D THA), which describes the real building up process of any cuboid by a FDM printer in the case of raster angle of 0 (90)° and filling ratio of 100%. Simulations were taken to investigate the influence of nozzle temperature, base plate temperature, environment temperature, layer thickness, printing speed, geometry dimension and the resolution of FDM printer on the temperature field,

and gradient variation with respect to space and time [100,113].

3.3.3 On structural performance

Statistical models have been used to establish a relationship between printing parameters (input variables) and mechanical behavior of FDM product (output response). Once established, it has been used as a tool to predict the mechanical properties based on input variables and, in turn, gain an optimization of FDM printing parameters. For instance, Ali and coworkers [114] proposed a two-factor-level Taguchi method for mechanical property optimization via design of experiments. Based on the analysis of mechanical properties derived from tests, the implementation of analysis of variance led to optimized printing variables for general use and for application/load-specific instances. Other statistical methods also have been applied for optimization of printing variables, such as polynomial regress model [115] and response surface methodology [116–118]. As being pointed out, the relationship of printing variables and their interactions and the manner in which they affect mechanical properties offers an insight to the feasibility of using FDM for rapid prototyping of products for practical implications.

For a part under real loads and fixtures, the common practice is to use finite element analysis for understanding how different printing parameters affect mechanical behavior of FDM products [18,119]. Yao and coworkers [120] proposed a method based on fracture mechanics for predicting the ultimate tensile strength (UTS) of FDM products. The factors influencing UTS included printing angle and layer thickness. By comparing the built micromechanical model with experimental data, it showed the relative residual sum of squares was all close to zero, indicating the model can accurately predict the UTS of FDM products for all angles and thickness.

In recent years, machine learning (ML) has been applied to aid solving the facing challenges from FDM, such as process control, process monitoring, and quality enhancement of FDM products [121,122]. For instance, Galatas and coworkers [39] applied the artificial neural network (ANN) to investigate the effect of FDM-printed-ABS core density and number of carbon fiber reinforced polymer layers on the mechanical properties. A nonlinear predictor based on ANN analysis was developed to predict the elastic modulus and specific strength of composite material. Due to good fast convergence, the three-term backpropagation was adopted to improve the elastic modulus and specific strength using far less training

data and less computational effort. Yanamandra and coworkers [123] applied ML of microstructure to obtain counterfeiting and unauthorized production of high-quality FDM parts for reverse engineers. With the help of the micro-CT (μCT) scan and scanning electronic microscope images, a refined recurrent neural network model achieved a high degree of accuracy in predicting fiber orientation within strands, which further was used to identify printing orientation at each layer of the FDM products.

4 Applications of FDM-printed devices

The FDM 3D devices are suitable for functional prototypes, tools, and low-volume manufacturing. FDM 3D printing technology has successfully provided some commercial solutions to industries, for example, customized cranial implant, customized kidney implant, COVID-19 breathing valve, customized mandibular implant, customized auto parts, flow pump body, industrial part model, customized running shoes, so on and so forth. Besides, Qi and coworkers [124] reported a multifunctional magnetorheological plastic containing PCL/TPU. This material has advantages in FDM printing, mechanical switching, shape memory, and self-healing. It has been used in the multifunctional magnetic sensitive materials, such as soft robots, medical care, and bionics and has broad application prospects. Sajadi and coworkers [125] reported tubulanes lattice polymer cubes using FDM technology. They made different kinds of cubes through computer simulation, and then used FDM technology to print polymer cubes by testing their structural properties. The results show that FDM technology can theoretically print cross-linked carbon nanotube-like tubulanes structures into physical parts, which have excellent strength. He and coworkers [126] reported a personalized triboelectric nanogenerator (TENG) layer based on FDM technology, which could be used to effectively harness vibration energy in environment. Although FDM has lower manufacturing accuracy compared with other 3D printing technologies, it has met the requirements of complex TENG devices.

The biomedical industry is already benefiting from FDM during recent years with the need for customizable, biocompatible, and sterilizable polymeric materials. It has to be admitted that every single patient or body has one's own unique needs. Given that, medical devices highly require the most customization of biomedical needs [127–130]. The traditional manufacturing makes the 3D products with high cost and most vital slow to produce. He and coworkers [131] reported the use of FDM technology to print PEEK nutcracker stents to treat nutcracker syndrome. Under laparoscopic surgery, his team implanted a PEEK porous venous extravascular stent "tailored" by FDM technology in advance for a patient with nutcracker syndrome. The patient recovered well after the operation. The stent did not cause any damage to the blood vessel during the review.

In terms of improving the mechanical properties of FDM devices, adding carbon nanotubes [132], graphene oxide [67], chopped carbon fibers [133], and other methods makes this technology extremely promising in transportation equipment, household goods, and medical industries. Topological optimization was also an efficient strategy for enhancing the mechanical properties [18,22,26,100]. In addition, FDM technology is used in the rapid manufacturing of polymer-based electronic devices [134], low-speed impact energy-absorbing structures [16], jewelry and fashion [135], optical devices [136], epidermal drug delivery polymerization microneedles [137], drone applications [39], bionic artificial bones [138], and other fields also have broad application prospects.

5 Conclusions

Except for the material itself, defects exist to limit the development of FDM. The faced challenges are to make FDM with more applicable materials, fast printing time, high dimensional accuracy, excellent surface quality, sufficient mechanical strength, so on and so forth. But the advantages of FDM technology in 3D printing are remarkable in new materials, new structures, new devices, and new functions. Indicated from the application of FDM 3D printing in cutting-edge fields, major technological breakthroughs have been achieved notably in research and development in the aerospace, commercial goods, and biomedical fields. With the development of 3D solid parts becoming more complex, precise, and multifunctional, FDM technology has shown a trend of high-resolution and fast printing.

Conflict of interest: The authors declare no conflict of interest regarding the publication of this paper.

References

[1] Chimene D, Kaunas R, Gaharwar A. Hydrogel bioink reinforcement for additive manufacturing: a focused review of emerging strategies. Adv Mater. 2020;32:1902026. doi: 10.1002/adma.201902026.

[2] Plocher J, Panesar A. Review on design and structural optimisation in additive manufacturing: towards next-generation lightweight structures. Mater Des. 2019;183:108164. doi: 10.1016/j.matdes.2019.108164.

[3] Culmone C, Smit G, Breedveld P. Additive manufacturing of medical instruments: a state-of-the-art review. Addit Manuf. 2019;27:461–73. doi: 10.1016/j.addma.2019.03.015.

[4] Paolini A, Kollmannsberger S, Rank E. Additive manufacturing in construction: a review on processes, applications, and digital planning methods. Addit Manuf. 2019;30:100894. doi: 10.1016/j.addma.2019.100894.

[5] Ngo T, Kashani A, Imbalzano G, Nguyen K, Hui D. Additive manufacturing (3d printing): a review of materials, methods, applications and challenges. Composites Part B. 2018;143:172–96. doi: 10.1016/j.compositesb.2018.02.012.

[6] Parandoush P, Lin D. A review on additive manufacturing of polymer–fiber composites. Compos Struct. 2017;182:36–53. doi: 10.1016/j.compstruct.2017.08.088.

[7] Kim H, Lin Y, Tseng T. A review on quality control in additive manufacturing. Rapid Prototyp J. 2018;24:645–69. doi: 10.1108/RPJ-03-2017-0048.

[8] Popescu D, Zapciu A, Amza C, Baciu F, Marinescu R. FDM process parameters influence over the mechanical properties of polymer specimens: a review. Polym Test. 2018;69:157–66. doi: 10.1016/j.polymertesting.2018.05.020.

[9] Gao M, Zheng F, Xu J, Zhang S, Bhosale S, Gu J, et al. Surface modification of nano-sized carbon black for reinforcement of rubber. Nanotechnol Rev. 2019;8:405–14. doi: 10.1515/ntrev-2019-0036.

[10] Pan Y, Xu K, Wu C. Recent progress in supercapacitors based on the advanced carbon electrodes. Nanotechnol Rev. 2019;8:299–314. doi: 10.1515/ntrev-2019-0029.

[11] Berger U. Aspects of accuracy and precision in the additive manufacturing of plastic gears. Virtual Phys Prototyp. 2015;10:49–57. doi: 10.1080/17452759.2015.1026127.

[12] Lu H, Liu Y, Leng J, Du S. Qualitative separation of the physical swelling effect on the recovery behavior of shape memory polymer. Eur Polym J. 2010;46:1908–14. doi: 10.1016/j.eurpolymj.2010.06.013.

[13] Lu H, Du S. A phenomenological thermodynamic model for the chemo-responsive shape memory effect in polymers based on flory-huggins solution theory. Polym Chem. 2014;5:1155–62. doi: 10.1039/C3PY01256E.

[14] Lei C. The research of key technologies of plastic particles 3d printer based on simulation. Harbin: Harbin Institute of Technology.

[15] Shrivastava A. Introduction to plastics engineering. Cambridge, MA, United States: William Andrew Publishing; 2018. doi: 10.1016/B978-0-323-39500-7.00009-5.

[16] Zhang P, Arceneaux DJ, Khattab A. Mechanical properties of 3D printed polycaprolactone honeycomb structure. J Appl Polym Sci. 2018;135:46018. doi: 10.1002/app.46018.

[17] Zhang P, Arceneaux D, Liu Z, Nikaeen P, Khattab A, Li G. A crack healable syntactic foam reinforced by 3D printed healing-agent based honeycomb. Composites Part B. 2018;151:25–34. doi: 10.1016/j.compositesb.2018.06.005.

[18] Hussey B, Nikaeen P, Dixon M, Akobi M, Khattab A, Cheng L, et al. Light-weight/defect-tolerant topologically self-interlocking polymeric structure by fused deposition modeling. Composites Part B. 2020;183:107700. doi: 10.1016/j.compositesb.2019.107700.

[19] Ramli M, Wahab M, Ahmad M, Bala A. FDM preparation of bio-compatible UHMWPE polymer for artificial implant. ARPN J Eng Appl Sci. 2016;11:5473–80.

[20] Rupinder S, Bedi P, Fraternali F, Ahuja I. Effect of single particle size, double particle size and triple particle size AL_2O_3 in nylon-6 matrix on mechanical properties of feed stock filament for FDM. Composites Part B. 2016;106:20–7. doi: 10.1016/j.compositesb.2016.08.039.

[21] Skowyra J, Pietrzak K, Alhnan M. Fabrication of extended-release patient-tailored prednisolone tablets via fused deposition modelling (FDM) 3D printing. Eur J Pharm Sci. 2015;68:11–7. doi: 10.1016/j.ejps.2014.11.009.

[22] Bates S, Farrow I, Trask R. 3D printed polyurethane honeycombs for repeated tailored energy absorption. Mater Des. 2016;112:172–83. doi: 10.1016/j.matdes.2016.08.062.

[23] Haque R, Chandran O, Lani S, Briand D. Self-powered triboelectric touch sensor made of 3D printed materials. Nano Energy. 2018;52:54–62. doi: 10.1016/j.nanoen.2018.07.038.

[24] Puigoriol-Forcada J, Alsina A, Salazar-Martin A, Gomez-Gras G, Perez M. Flexural fatigue properties of polycarbonate fused-deposition modelling specimens. Mater Des. 2018;155:414–21. doi: 10.1016/j.matdes.2018.06.018.

[25] Compton B, Lewis J. 3D printing of lightweight cellular composites. Adv Mater. 2014;26:5930–5. doi: 10.1002/adma.201401804.

[26] Wu W, Geng P, Li G, Zhao D, Zhang H, Zhao J. Influence of layer thickness and raster angle on the mechanical properties of 3D-printed PEEK and a comparative mechanical study between PEEK and ABS. Mater. 2015;8:5834–46. doi: 10.3390/ma8095271.

[27] Rinaldi M, Ghidini T, Cecchini F, Brandao A, Nanni F. Additive layer manufacturing of poly(ether ether ketone) via FDM. Composites Part B. 2018;145:162–72. doi: 10.1016/j.compositesb.2018.03.029.

[28] Arif M, Kumar S, Varadarajan K, Cantwell W. Performance of biocompatible PEEK processed by fused deposition additive manufacturing. Mater Des. 2018;146:249–59. doi: 10.1016/j.matdes.2018.03.015.

[29] Zhao F, Li D, Jin Z. Preliminary investigation of poly-ether-ether-ketone based on fused deposition modeling for medical applications. Materials. 2018;11:288. doi: 10.3390/ma11020288.

[30] Berretta S, Evans K, Ghita O. Additive manufacture of PEEK cranial implants: manufacturing considerations versus

accuracy and mechanical performance. Mater Des. 2018;139:141–52. doi: 10.1016/j.matdes.2017.10.078.

[31] Lee K, Park H, Kim J, Chun D. Fabrication of a superhydrophobic surface using a fused deposition modeling (FDM) 3D printer with poly lactic acid (PLA) filament and dip coating with silica nanoparticles. Appl Surf Sci. 2019;467:979–91. doi: 10.1016/j.apsusc.2018.10.205.

[32] Wu T, Tong Y, Qiu F, Yuan D, Zhang G, Qu J. Morphology, rheology property, and crystallization behavior of PLLA/OMMT nanocomposites prepared by an innovative eccentric rotor extruder. Polym Adv Technol. 2018;29:41–51. doi: 10.1002/pat.4087.

[33] Tao Y, Wang H, Li Z, Li P, Shi S. Development and application of wood flour-filled polylactic acid composite filament for 3D printing. Mater. 2017;10:339. doi: 10.3390/ma10040339.

[34] Daver F, Lee K, Brandt M, Shanks R. Cork-pla composite fifilaments for fused deposition modelling. Compos Sci Technol. 2018;168:230–7. doi: 10.1016/j.compscitech.2018.10.008.

[35] Hanon M, Alshammas Y, Zsidai L. Effect of print orientation and bronze existence on tribological and mechanical properties of 3D-printed bronze/pla composite. Int J Adv Manuf Technol. 2020;108:553–70. doi: 10.1007/s00170-020-05391-x.

[36] Nikzad M, Masood S, Sbarski I. Thermo-mechanical properties of a highly filled polymeric composites for fused deposition modeling. Mater Des. 2011;32:3448–56. doi: 10.1016/j.matdes.2011.01.056.

[37] Bose S, Vahabzadeh S, Bandyopadhyay A. Bone tissue engineering using 3D printing. Mater Des. 2013;16:496–504. doi: 10.1016/j.mattod.2013.11.017.

[38] Quan Z, Larimore Z, Wu A, Yu J, Qin X, Mirotznik M, et al. Microstructural design and additive manufacturing and characterization of 3D orthogonal short carbon fiber/acrylonitrile-butadiene-styrene preform and composite. Compos Sci Technol. 2016;126:139–48. doi: 10.1016/j.compscitech.2016.02.021.

[39] Galatas A, Hassanin H, Zweiri Y, Seneviratne L. Additive manufactured sandwich composite/ABS parts for unmanned aerial vehicle applications. Polymers. 2018;10:1262–78. doi: 10.3390/polym10111262.

[40] Gao X, Zhang D, Qi S, Wen X, Su Y. Mechanical properties of 3D parts fabricated by fused deposition modeling: effect of various fillers in polylactide. J Appl Polym Sci. 2019;136:10. doi: 10.1002/app.47824.

[41] Paul D, Robeson L. Polymer nanotechnology: nanocomposites. Polym. 2008;49:3187–204. doi: 10.1016/j.polymer.2008.04.017.

[42] Lu H, Liang F, Gou J. Nanopaper enabled shape-memory nanocomposite with vertically aligned nickel nanostrand: controlled synthesis and electrical actuation. Soft Matter. 2011;7:7416–23. doi: 10.1039/C1SM05765K.

[43] Li Z, Xu K, Pan Y. Recent development of supercapacitor electrode based on carbon materials. Nanotechnol Rev. 2019;8:35–49. doi: 10.1515/ntrev-2019-0004.

[44] Lu H, Huang W. Synergistic effect of self-assembled carboxylic acid-functionalized carbon nanotubes and carbon fiber for improved electro-activated polymeric shape-memory nanocomposite. Appl Phys Lett. 2013;102:231910. doi: 10.1063/1.4811134.

[45] Pantic S, Skodric S, Loncar Z, Pantic I. Zinc oxide nanoparticles: potential novel applications in cellular physiology, pathology, neurosciences and cancer research. Rev Adv Mater Sci. 2019;58:17–21. doi: 10.1515/rams-2019-0002.

[46] Pantic S, Skodric S, Loncar Z, Pantic I. Neurotoxocity, nephrotoxicity, and hepatotoxicity of copper-based nanoparticles: potential implications in molecular medicine and neurosciences. Rev Adv Mater Sci. 2019;58:201–5. doi: 10.1515/rams-2019-0032.

[47] Power A, Gorey B, Chandra S, Chapman J. Carbon nanomaterials and their application to electrochemical sensors: a review. Nanotechnol Rev. 2018;7:19–41. doi: 10.1515/ntrev-2017-0160.

[48] Alexander M, Dubois P. Polymer-layered silicate nanocomposites: preparation, properties and uses of a new class of materials. Mater Sci Eng R Rep. 2000;28:1–63. doi: 10.1016/S0927-796X(00)00012-7.

[49] Muller K, Bugnicourt E, Latorre M, Jorda M, Echegoyen S, Lagaron J, et al. Review on the processing and properties of polymer nanocomposites and nanocoatings and their applications in the packaging, automotive and solar energy fields. Nanomater. 2017;7:74. doi: 10.3390/nano7040074.

[50] Liu Z, Wang Y, Shi J. Tensile performance of fused deposition modeling PA 6 polymer composites with nanoparticle reinforcement and/or continuous fiber reinforcement. J Micro Nanomanuf. 2019;9:041001. doi: 10.1115/1.4044913.

[51] Vidakis N, Petousis M, Savvakis K, Maniadi A, Koudoumas E. A comprehensive investigation of the mechanical behavior and the dielectrics of pure polylactic acid (PLA) and PLA with graphene (GNP) in fused deposition modeling (FDM). Int J Plast Technol. 2019;23:195–206. doi: 10.1007/s12588-019-09248-1.

[52] Wang Q, Ji C, Sun L, Sun J, Liu J. Cellulose nanofibrils filled poly(lactic acid) biocomposite filament for fdm 3D printing. Molecules. 2020;25:2319. doi: 10.3390/molecules25102319.

[53] Kim H, Ryu K, Baek D, Khan T, Kim H, Shin S, et al. 3D printing of polyethylene terephthalate glycol-sepiolite composites with nanoscale orientation. ACS Appl Mater Interfaces. 2020;12:23453–63. doi: 10.1021/acsami.0c03830.

[54] Woosley S, Galehdari N, Kelkar A, Aravamudhan S. Fused deposition modeling 3D printing of boron nitride composites for neutron radiation shielding. J Mater Res. 2018;33:3657–64. doi: 10.1557/jmr.2018.316.

[55] Dul S, Fambri L, Pegoretti A. Filaments production and fused deposition modelling of ABS/carbon nanotubes composites. Nanomater. 2018;8:49. doi: 10.3390/nano8010049.

[56] Zhang W, Cotton C, Sun J, Heider D, Gu B, Sun B, et al. Interfacial bonding strength of short carbon fiber/acrylonitrile-butadiene-styrene composites fabricated by fused deposition modeling. Composites Part B. 2018;137:51–9. doi: 10.1016/j.compositesb.2017.11.018.

[57] Cobos C, Fenollar O, Martinez J, Ferrandiz S, Garzon L. Effect of maleinized linseed oil (MLO) on thermal and rheological properties of PLA/MWCNT and PLA/HNT nanocomposites for additive manufacturing. Rapid Prototyp J. 2020;26:1027–33. doi: 10.1108/RPJ-08-2019-0217.

[58] Bustillos J, Montero D, Nautiyal P, Loganathan A, Boesl B, Agarwal A. Integration of graphene in poly (lactic) acid by 3D printing to develop creep and wearresistant hierarchical

nanocomposites. Polym Compos. 2018;39:3877–88. doi: 10.1002/pc.24422.

[59] Prashantha K, Roger F. Multifunctional properties of 3D printed poly (lactic acid)/graphene nanocomposites by fused deposition modeling. J Macromol Sci A. 2017;54:24–9. doi: 10.1080/10601325.2017.1250311.

[60] Zhang F, Wei M, Viswanathan V, Swart B, Shao Y, Wu G, et al. 3D printing technologies for electrochemical energy storage. Nano Energy. 2017;40:418–31. doi: 10.1016/j.nanoen.2017.08.037.

[61] Gonçalves J, Lima P, Krause B, Pötschke P, Lafont U, Gomes J, et al. Electrically conductive polyetheretherketone nanocomposite filaments: from production to fused deposition modeling. Polymers. 2018;10:925. doi: 10.3390/polym10080925.

[62] Kwon S, Kim S, Kim I, Hong Y, Na S. Direct 3D printing of graphene nanoplatelet/silver nanoparticlebased nanocomposites for multiaxial piezoresistive sensor applications. Adv Mater Technol. 2018;4:1800500. doi: 10.1002/admt.201800500.

[63] Ivanov E, Kotsilkova R, Xia H, Chen Y, Donato R, Donato K, et al. PLA/graphene/MWCNT composites with improved electrical and thermal properties suitable for FDM 3D printing applications. Appl Sci. 2019;9:1209. doi: 10.3390/app9061209.

[64] Shmueli Y, Lin Y, Zuo X, Guo Y, Lee S, Freychet G, et al. In situ X-ray scattering study of isotactic polypropylene/graphene nanocomposites under shear during fused deposition modeling 3D printing. Compos Sci Technol. 2020;196:108227. doi: 10.1016/j.compscitech.2020.108227.

[65] Yang L, Chen Y, Wang M, Shi S, Jing J. Fused deposition modeling 3D printing of novel poly(vinyl alcohol)/graphene nanocomposite with enhanced mechanical and electromagnetic interference shielding properties. Ind Eng Chem Res. 2020;59:8066–77. doi: 10.1021/acs.iecr.0c00074.

[66] Zhu D, Ren Y, Liao G, Jiang S, Liu F, Guo J, et al. Thermal and mechanical properties of polyamide 12/graphene nanoplatelets nanocomposites and parts fabricated by fused deposition modeling. J Appl Polym Sci. 2017;134:45332. doi: 10.1002/app.45332.

[67] Chen Q, Mangadlao J, Wallat D, Leon A, Pokorski J, Advincula R. 3D printing biocompatible polyurethane/poly (lactic acid)/graphene oxide nanocomposites: anisotropic properties. ACS Appl Mater Interfaces. 2017;9:4015–23. doi: 10.1021/acsami.6b11793.

[68] Dorigato A, Moretti V, Dul S, Unterberger S, Pegoretti A. Electrically conductive nanocomposites for fused deposition modelling. Synth Met. 2017;226:7–14. doi: 10.1016/j.synthmet.2017.01.009.

[69] Singh D, Singh R, Boparai K. Development and surface improvement of FDM pattern based investment casting of biomedical implants: a state of art review. J Manuf Process. 2018;31:80–95. doi: 10.1016/j.jmapro.2017.10.026.

[70] Zhao Y, Yang J, Ding X, Ding X, Duan S, Xu F. Polycaprolactone/polysaccharide functional composites for low-temperature fused deposition modelling. Bioact Mater. 2020;5:185–91. doi: 10.1016/j.bioactmat.2020.02.006.

[71] Mohamed O, Masood S, Bhowmik J. Optimization of fused deposition modeling process parameters: a review of current research and future prospects. J Adv Manuf. 2015;3:42–53. doi: 10.1007/s40436-014-0097-7.

[72] Mohan N, Senthil P, Vinodh S, Jayanth N. A review on composite materials and process parameters optimisation for the fused deposition modelling process. Virtual Phys Prototyp. 2017;12:47–59. doi: 10.1080/17452759.2016.1274490.

[73] Carrell J, Gruss G, Gomez E. Four-dimensional printing using fused-deposition modeling: a review. Rapid Prototyp J. 2020;26:855–69. doi: 10.1108/RPJ-12-2018-0305.

[74] Gosselin C, Duballet R, Roux P, Gaudilliere N, Dirrenberger J, Morel P. Large-scale 3D printing of ultra-high performance concrete-a new processing route for architects and builders. Mater Des. 2016;100:102–9. doi: 10.1016/j.matdes.2016.03.097.

[75] Duty C, Kunc V, Compton B, Post B, Erdman D, Smith R, et al. Structure and mechanical behavior of big area additive manufacturing (BAAM). Mater Rapid Prototyp J. 2017;23:181–9. doi: 10.1108/RPJ-12-2015-0183.

[76] Jones R, Haufe P, Sells E, Iravani P, Olliver V, Palmer C, et al. Reprap-the replicating rapid prototyper. Robotica. 2011;29:177–91. doi: 10.1017/S026357471000069X.

[77] Solomon I, Sevvel P, Gunasekaran J. A review on the various processing parameters in FDM. Mater Today Proc. 2020. doi: 10.1016/j.matpr.2020.05.484.

[78] Tlegenov Y, Wong Y, Hong G. A dynamic model for nozzle clog monitoring in fused deposition modelling. Rapid Prototyp J. 2017;23:391–400. doi: 10.1108/RPJ-04-2016-0054.

[79] Go J, Schiffres S, Stevens A, Hart A. Rate limits of additive manufacturing by fused filament fabrication and guidelines for high-throughput system design. Addit Manuf. 2017;16:1–11. doi: 10.1016/j.addma.2017.03.007.

[80] Go J, Hart A. Fast desktop-scale extrusion additive manufacturing. Addit Manuf. 2017;18:276–84. doi: 10.1016/j.addma.2017.10.016.

[81] Li F, Macdonald N, Guijt R, Breadmore M. Increasing the functionalities of 3D printed microchemical devices by single material, multimaterial, and print-pause-print 3D printing. Lab Chip. 2019;19:35–49. doi: 10.1039/C8LC00826D.

[82] Truby R, Lewis J. Printing soft matter in three dimensions. Nature. 2016;540:371–8. doi: 10.1038/nature21003.

[83] Everything about nozzles with a different diameter. URL https://blog.prusaprinters.org/everything-about-nozzles-with-a-different-diameter_8344/.

[84] Silveira Z, Freitas M, Inforcatti N, Noritomi P, Silva J. Design development and functional validation of an interchangeable head based on mini screw extrusion applied in an experimental desktop 3-D printer. Int J Rapid Manuf. 2014;4:49–65. doi: 10.1504/IJRAPIDM.2014.062037.

[85] Tseng J, Liu C, Yen Y, Belkner J, Bremicker T, Liu B, et al. Screw extrusion-based additive manufacturing of PEEK. Mater Des. 2018;140:209–21. doi: 10.1016/j.matdes.2017.11.032.

[86] Cai L, Wang Y, Liu Z, Cheng Q. Carrying capacity analysis and optimizing of hydrostatic slider bearings under inertial force and vibration impact using finite difference method (FDM). J Vibroeng. 2015;17:2781–94.

[87] Hertle S, Drexler M, Drummer D. Additive manufacturing of poly(propylene) by means of melt extrusion. Macromol Mater Eng. 2016;301:1482–93. doi: 10.1002/mame.201600259.

[88] Roopavath U, Malferrari S, Haver A, Verstreken F, Rath S, Kalaskar D. Optimization of extrusion based ceramic 3D printing process for complex bony designs. Mater Des. 2019;162:263–70. doi: 10.1016/j.matdes.2018.11.054.

[89] Zhang P, Li G. Structural relaxation behavior of strain hardened shape memory polymer fibers for self-healing applications. J Polym Sci B Polym Phys. 2013;51:966–77. doi: 10.1002/polb.23295.

[90] Wei C, Dong J. Direct fabrication of high-resolution three-dimensional polymeric scaffolds using electrohydrodynamic hot jet plotting. J Microm Microeng. 2013;23:025017. doi: 10.1088/0960-1317/23/2/025017.

[91] Zhang B, Seong B, Nguyen V, Byun D. 3D printing of high-resolution pla-based structures by hybrid electrohydrodynamic and fused deposition modeling techniques. J Micromech Microeng. 2016;26:025015. doi: 10.1088/0960-1317/26/2/025015.

[92] He J, Xia P, Li D. Development of melt electrohydrodynamic 3D printing for complex microscale poly(ϵ-caprolactone) scaffolds. Biofabrication. 2016;8:035008. doi: 10.1088/1758-5090/8/3/035008.

[93] Vijayavenkataraman S, Zhang S, Lu W, Fuh J. Electrohydrodynamic-jetting (EHD-jet) 3D-printed functionally graded scaffolds for tissue engineering applications. J Micromech Microeng. 2018;33:1999–2011. doi: 10.1557/jmr.2018.159.

[94] Liu H, Vijayavenkataraman S, Wang D, Jing L, Sun J, He K. Influence of electrohydrodynamic jetting parameters on the morphology of PCL scaffolds. Int J Bioprint. 2017;3:72–82. doi: 10.18063/IJB.2017.01.009.

[95] Wang H, Vijayavenkataraman S, Wu Y, Shu Z, Sun J, Hsi J. Investigation of process parameters of electrohydrodynamic jetting for 3D printed PCL fibrous scaffolds with complex geometries. Int J Bioprint. 2016;2:02005. doi: 10.18063/IJB.2016.01.005.

[96] Wu S, Li J, Mai J, Chang M. Three-dimensional electrohydrodynamic printing and spinning of flexible composite structures for oral multidrug forms. ACS Appl Mater Interfaces. 2018;10:24876–85. doi: 10.1021/acsami.8b08880.

[97] Li J. Numerical simulation and experimental study on fused deposition of pla-nha-based biomimetic artificial bone material. Harbin: Harbin Institute of Technology.

[98] Ahn D, Kweon J, Choi J, Lee S. Relation between surface roughness and overlap interval in fused deposition modeling. Adv Mater Res. 2011;264:1625–30. doi: 10.4028/www.scientific.net/AMR.264-265.1625.

[99] Costa S, Duarte F, Covas J. Thermal conditions affecting heat transfer in FDM/FFE: a contribution towards the numerical modelling of the process. Virtual Phys Prototyp. 2015;10:35–46. doi: 10.1080/17452759.2014.984042.

[100] Zhang J, Wang X, Yu W, Deng Y. Numerical investigation of the influence of process conditions on the temperature variation in fused deposition modeling. Mater Des. 2017;130:59–68. doi: 10.1016/j.matdes.2017.05.040.

[101] Turner B, Strong R, Gold S. A review of melt extrusion additive manufacturing processes: I. Process design and modeling. Rapid Prototyp J. 2014;20:192–204. doi: 10.1108/RPJ-01-2013-0012.

[102] Bikas H, Stavropoulos P, Chryssolouris G. Additive manufacturing methods and modelling approaches: a critical review. Int J Adv Manuf Technol. 2016;83:389–405. doi: 10.1007/s00170-015-7576-2.

[103] Comminal R, Serdeczny M, Pedersen D, Spangenberg J. Numerical modeling of the strand deposition flow in extrusion-based additive manufacturing. Addit Manuf. 2018;20:68–76. doi: 10.1016/j.addma.2017.12.013.

[104] Bellehumeur C, Li L, Sun Q, Gu P. Modeling of bond formation between polymer filaments in the fused deposition modeling process. J Manuf Process. 2004;6:170–8. doi: 10.1016/S1526-6125(04)70071-7.

[105] Zhang P, Li G. Advances in healing-on-demand polymers and polymer composites. Prog Polym Sci. 2016;57:32–63. doi: 10.1016/j.progpolymsci.2015.11.005.

[106] Guo C, Zhang M, Bhandari B. Model building and slicing in food 3D printing processes: a review. Compr Rev Food Sci Food Saf. 2019;18:1052–69. doi: 10.1111/1541-4337.12443.

[107] Gordelier T, Thies P, Turner L, Johanning L. Optimising the FDM additive manufacturing process to achieve maximum tensile strength: a state-of-the-art review. Rapid Prototyp J. 2019;25:953–71. doi: 10.1108/RPJ-07-2018-0183.

[108] Vyavahare S, Teraiya S, Panghal D, Kumar S. Fused deposition modelling: a review. Rapid Prototyp J. 2020;26:176–201. doi: 10.1108/RPJ-04-2019-0106.

[109] Coogan T, Kazmer D. Healing simulation for bond strength prediction of FDM. Rapid Prototyp J. 2017;23:551–61. doi: 10.1108/RPJ-03-2016-0051.

[110] Zhou X, Hsieh S, Sun Y. Experimental and numerical investigation of the thermal behaviour of polylactic acid during the fused deposition process. Virtual Phys Prototyp. 2017;12:221–33. doi: 10.1080/17452759.2017.1317214.

[111] Xia H, Lu J, Dabiri S, Tryggvason G. Fully resolved numerical simulations of fused deposition modeling. Part I: fluid flow. Rapid Prototyp J. 2018;24:463–76. doi: 10.1108/RPJ-12-2016-0217.

[112] Xia H, Lu J, Tryggvason G. Fully resolved numerical simulations of fused deposition modeling. Part II-solidification, residual stresses and modeling of the nozzle. Rapid Prototyp J. 2018;24:973–87. doi: 10.1108/RPJ-11-2017-0233.

[113] Yin J, Lu C, Fu J, Huang Y, Zheng Y. Interfacial bonding during multi-material fused deposition modeling (FDM) process due to inter-molecular diffusion. Mater Des. 2018;150:104–12. doi: 10.1016/j.matdes.2018.04.029.

[114] Torres J, Cole M, Owji A, DeMastry Z, Gordon A. An approach for mechanical property optimization of fused deposition modeling with polylactic acid via design of experiments. Rapid Prototyp J. 2016;22:387–404. doi: 10.1108/RPJ-07-2014-0083.

[115] Wang X, Akobi M, Nikaeen P, Khattab A, He T, Li J, et al. Modeling and statistical understanding: the effect of cnt on mechanical properties of recycled polycaprolactone/epoxy composites. J Appl Polym Sci. 2021;138(22):49886. doi: 10.1002/app.20200748.

[116] Zhang P, Khattab A. Characteristics of process-induced properties in carbon nanofiber aqueous dispersion. Micro Nano Lett. 2018;13:524–9. doi: 10.1049/mnl.2017.0585.

[117] Shou W, Zhang P, Khattab A. Parametric study of an automated nanoparticles spray system for nanofibers/fabric reinforced composites. Polym Compos. 2018;40:1068–77. doi: 10.1002/pc.24797.

[118] Zhang P, Akobi M, Khattab A. Recyclability/malleability of crack healable polymer composites by response surface methodology. Composites Part B. 2019;168:129–39. doi: 10.1016/j.compositesb.2018.12.048.

[119] Domingo-Espin M, Puigoriol-Forcada J, Garcia-Granada A, Lluma J, Borros S, Reyes G. Mechanical property characterization and simulation of fused deposition modeling polycarbonate parts. Mater Des. 2015;83:670–7. doi: 10.1016/j.matdes.2015.06.074.

[120] Yao T, Deng Z, Zhang K, Li S. A method to predict the ultimate tensile strength of 3D printing polylactic acid (PLA) materials with different printing orientations. Composites Part B. 2019;163:393–402. doi: 10.1016/j.compositesb.2019.01.025.

[121] Baumann F, Sekulla A, Hassler M, Himpel B, Pfeil M. Trends of machine learning in additive manufacturing. Int J Rapid Manuf. 2018;7:310–36. doi: 10.1504/IJRAPIDM.2018.095788.

[122] Goh G, Sing S, Yeong W. A review on machine learning in 3D printing: applications, potential, and challenges. Artif Intell Rev. 2020;1–32. doi: 10.1007/s10462-020-09876-9.

[123] Yanamandra K, Chen G, Xu X, Mac G, Gupta N. Reverse engineering of additive manufactured composite part by toolpath reconstruction using imaging and machine learning. Compos Sci Technol. 2020;198:108318. doi: 10.1016/j.compscitech.2020.108318.

[124] Qi S, Fu J, Xie Y, Li Y, Gan R, Yu M. Versatile magnetorheological plastomer with 3D printability, switchable mechanics, shape memory, and self-healing capacity. Compos Sci Technol. 2019;183:107817. doi: 10.1016/j.compscitech.2019.107817.

[125] Sajadi S, Woellner C, Ramesh P, Eichmann S, Sun Q, Boul P, et al. 3D printed tubulanes as lightweight hypervelocity impact resistant structures. Small. 2019;15:1904747. doi: 10.1002/smll.201904747.

[126] He S, Yu Z, Zhou H, Huang Z, Zhang Y, Li Y, et al. Polymer tubes as carrier boats of thermosetting and powder materials based on 3D printing for triboelectric nanogenerator with microstructure. Nano Energy. 2018;52:134–41. doi: 10.1016/j.nanoen.2018.07.044.

[127] Chohan J, Singh R. Pre and post processing techniques to improve surface characteristics of FDM parts: a state of art review and future applications. Rapid Prototyp J. 2017;23:495–513. doi: 10.1108/RPJ-05-2015-0059.

[128] Singh D, Singh R, Boparai K, Farina I, Feo L, Verma A. *In vitro* studies of SS 316 L biomedical implants prepared by FDM, vapor smoothing and investment casting.

Composites Part B. 2018;132:107–14. doi: 10.1016/j.compositesb.2017.08.019.

[129] Tiwary V, Arunkumar P, Deshpande A, Rangaswamy N. Surface enhancement of FDM patterns to be used in rapid investment casting for making medical implants. Rapid Prototyp J. 2019;25:904–14. doi: 10.1108/RPJ-07-2018-0176.

[130] Li Y, Feng Z, Hao L, Huang L, Xin C, Wang Y, et al. A review on functionally graded materials and structures via additive manufacturing: from multiscale design to versatile functional properties. Adv Mater Technol. 2020;5:1900981. doi: 10.1002/admt.201900981.

[131] He D, Liang J, Wang H, Jiao Y, Wu B, Cui D, et al. 3D-printed PEEK extravascular stent in the treatment of nutcracker syndrome: imaging evaluation and short-term clinical outcome. Front Bioeng Biotechnol. 2020;8:732. doi: 10.3389/fbioe.2020.00732.

[132] Calderon-Villajos R, Lopez A, Peponi L, Manzano-Santamaria J, Urena A. 3D-printed self-healing composite polymer reinforced with carbon nanotubes. Mater Lett. 2019;249:91–4. doi: 10.1016/j.matlet.2019.04.069.

[133] Ferreira R, Amatte I, Dutra T, Burger D. Experimental characterization and micrography of 3D printed PLA and PLA reinforced with short carbon fibers. Composites Part B. 2017;124:88–100. doi: 10.1016/j.compositesb.2017.05.013.

[134] Chen G, Chen N, Wang Q. Preparation of poly(vinyl alcohol)/ionic liquid composites with improved processability and electrical conductivity for fused deposition modeling. Mater Des. 2018;157:273–83. doi: 10.1016/j.matdes.2018.07.054.

[135] Zarek M, Layani M, Eliazar S, Mansour N, Cooperstein I, Shukrun E, et al. 4D printing shape memory polymers for dynamic jewellery and fashionwear. Virtual Phys Prototyp. 2016;11:263–70. doi: 10.1080/17452759.2016.1244085.

[136] Torrada A, Roberson D. Failure analysis and anisotropy evaluation of 3D-printed tensile test specimens of different geometries and print raster patterns. J Fail Anal Prev. 2016;116:154–64. doi: 10.1007/s11668-016-0067-4.

[137] Luzuriaga M, Berry D, Reagan J, Smaldone R, Gassensmith J. Biodegradable 3D printed polymer microneedles for transdermal drug delivery. Lab Chip. 2013;18:1223–30. doi: 10.1039/C8LC00098K.

[138] Xu N, Ye X, Wei D, Zhong J, Chen Y, Xu G, et al. 3D artificial bones for bone repair prepared by computed tomography-guided fused deposition modeling for bone repair. ACS Appl Mater Interfaces. 2014;6:14952–63. doi: 10.1021/am502716t.